Molecular Crystals and Liquid Crystals

Publication details, including instructions for authors and subscription information:
http://www.tandfonline.com/loi/gmcl20

Low Surface Energy Characteristics of Mesophase-Forming ABC and ACB Triblock Copolymers with Fluorinated B Blocks

G. Galli [a], E. Martinelli [a], E. Chiellini [a], C. K. Ober [b] & A. Glisenti [c]

[a] Dipartimento di Chimica e Chimica Industriale, UdR Pisa INSTM, Università di Pisa, via Risorgimento Pisa, Italy

[b] Department of Materials Science and Engineering, Cornell University, Ithaca, NY, USA

[c] Dipartimento di Chimica Inorganica, Metallorganica ed Analitica, Università di Padova, Padova, Italy

Version of record first published: 17 Oct 2011

To cite this article: G. Galli, E. Martinelli, E. Chiellini, C. K. Ober & A. Glisenti (2005): Low Surface Energy Characteristics of Mesophase-Forming ABC and ACB Triblock Copolymers with Fluorinated B Blocks, Molecular Crystals and Liquid Crystals, 441:1, 211-226

To link to this article: http://dx.doi.org/10.1080/154214091009770

Mol. Cryst. Liq. Cryst., Vol. 441, pp. 211–226, 2005

ISSN: 1542-1406 print/1563-5287 online
DOI: 10.1080/154214091009770

Taylor & Francis
Taylor & Francis Group

Low Surface Energy Characteristics of Mesophase-Forming ABC and ACB Triblock Copolymers with Fluorinated B Blocks

G. Galli
E. Martinelli
E. Chiellini
Dipartimento di Chimica e Chimica Industriale, UdR Pisa INSTM, Università di Pisa, via Risorgimento Pisa, Italy

C. K. Ober
Department of Materials Science and Engineering, Cornell University, Ithaca, NY, USA

A. Glisenti
Dipartimento di Chimica Inorganica, Metallorganica ed Analitica, Università di Padova, Padova, Italy

We prepared several triblock copolymers of the A–B–C and A–C–B types composed of hydrophobic polystyrene (A), hydrophobic/lipophobic fluorinated polystyrene (B), and hydrophilic PEG-modified polystyrene (C) blocks with greatly varied degrees of polymerization. The resulting surface structure and organization of the polymer films were investigated by measurements of the static contact angle with several interrogating liquids and by X-ray photoelectron spectroscopy at different take-off angles. The contact angle values were also used to evaluate the film surface tensions, following two fundamentally different approaches. The low surface energies found for any of the triblock copolymers were attributed to the pronounced hydrophobicity and lipophobicity of the outermost surface caused by the preferential segregation of the fluorinated block regardless of the distinctly different macromolecular architectures of the triblock copolymers.

Keywords: block copolymer; contact angle; fluorinated polymer; mesophase; surface energy

We are grateful to the Italian MIUR (PRIN 2003-03-0237) and the European Union (HPRN-CT-2002-00202, *SAMPA*) for financial support of the work. We also thank E. J. Kramer (UCSB) for helpful discussions.

Address correspondence to G. Galli, Dipartimento di Chimica e Chimica Industriale, UdR Pisa INSTM, Università di Pisa, via Risorgimento 35, 56126 Pisa, Italy. E-mail: gallig@dcci.unipi.it

INTRODUCTION

Control of the surface properties of polymeric materials by means of self-organization is a major objective of current science and technology. Such self-organization can be driven by several mechanisms including phase separation of block copolymers, liquid crystallinity, hydrogen bonding, and surface segregation. Combinations of mechanisms may be used to form an ordered surface structure. As one example, block copolymers microphase separate to a preferred microstructure, but when low surface energy blocks are incorporated, surface and interface segregation will also take place to enhance further organization in the region of the low energy surface [1].

Polymers incorporating fluorinated side groups are typically low surface energy materials [2]. When mesogenic, rodlike fluorinated chains are introduced in the side groups their ordering in a smectic mesophase *at the surface* can provide an additional means to create non-reconstructing, long-lasting low energy surfaces [1,3]. Uses that are diverse as lubrication, wear control, antisoiling and anti(bio)fouling may become viable by taking advantage of such molecular and macromolecular designs.

We are interested in the synthesis and study of diverse architectures of mesophase-forming fluorinated polymers [4], including block copolymers with different philic/phobic constituent blocks [1,5]. In this work we investigated several triblock copolymers with greatly different phobic polymer blocks and show that their mutual incompatibility enhances surface segregation and provides low energy surfaces.

EXPERIMENTAL PART

Monomers

The monomers SF8 [6] and SP3 [7] were synthesized according to general literature procedures from 4-chloromethylstyrene and 1H,1H,2H,2H-perfluorodecanol (F8) and triethyleneglycol monomethyl ether (P3), respectively. Styrene (from Fluka) (S) was washed with 10% NaOH, water, dried on $MgSO_4$, and distilled under vacuum prior to use.

TEMPO-Terminated Polystyrene Poly(S)

A Pyrex vial was charged with 6.00 g (57.6 mmol) of monomer S, 63 mg (0.26 mmol) of benzoyl peroxide (BPO), 64 mg (0.42 mmol) of 2,2,6,6-tetramethyl-1-piperidinyloxide (TEMPO) and 30 mg (0.11 mmol) of 2-fluoro-1-methylpyridinium-4-toluenesulfonate (FMPTS). After degassing by freeze-thaw cycles, the vial was sealed and the reaction was let to proceed at 85°C for 2 h and then for 24 h at

125°C. The polymer was purified by repeated precipitations from chloroform into methanol. Yield 26%.

TEMPO-Terminated Diblock Copolymer Poly(S-b-SF8)

A Pyrex vial was charged with 76 mg ($6.8 \cdot 10^{-3}$ TEMPO mmol) of poly(S), 0.80 g (1.38 mmol) of monomer SF8 and 4 ml of diglyme. After degassing by freeze-thaw cycles, the vial was sealed and the reaction was let to proceed for 154 h at 125°C. The polymer was purified by repeated precipitations from trichloro-trifluoroethane/chloroform (1:1 v/v) into methanol and then extracted with acetone at room temperature overnight. Yield 48%.

TEMPO-Terminated Diblock Copolymers Poly(S-b-SP3)

In a typical preparation of poly(S-*b*-SP3)c, a Pyrex vial was charged with 162 mg ($1.5 \cdot 10^{-2}$ TEMPO mmol) of poly(S), 1.00 g (3.57 mmol) of monomer SP3 and 3 ml of diglyme. After degassing by freeze-thaw cycles, the vial was sealed and the reaction was let to proceed for 72 h at 125°C. The polymer was purified by repeated precipitations from acetone into n-hexane and then extracted with cyclohexane at room temperature for 24 h. Yield 62%.

Triblock Copolymers Poly(S-b-SF8-b-SP3)

In a typical preparation of poly(S-*b*-SF8-*b*-SP3)a, a Pyrex vial was charged with 90 mg ($1.3 \cdot 10^{-3}$ TEMPO mmol) of poly(S-*b*-SF8), 0.61 g (2.2 mmol) of monomer SP3 and 8 ml of diglyme. After degassing by freeze-thaw cycles, the vial was sealed and the reaction was let to proceed for 134 h at 125°C. The polymer was purified by repeated precipitations from trifluorotoluene/chloroform (1:1 v/v) into methanol. Yield 11%.

Triblock Copolymers Poly(S-b-SP3-b-SF8)

In a typical preparation of poly(S-*b*-SP3-*b*-SF8)c, a Pyrex vial was charged with 128 mg ($2.0 \cdot 10^{-3}$ TEMPO mmol) of poly(S-*b*-SP3)c, 0.52 g (0.9 mmol) of monomer SF8 and 4 ml of diglyme. After degassing by freeze-thaw cycles, the vial was sealed and the reaction was let to proceed for 86 h at 125°C. The polymer was precipitated into cyclohexane and then extracted with cyclohexane at room temperature for 48 h. Yield 28%.

FT-IR (KBr, $\bar{\nu}$ in cm^{-1}) 3050–3020 (νC−H aromatic), 2920 (νCH_2), 1600–1450 (νC=C aromatic), 1240–1020 (νC−O−C and C−F), 703 (δC−H aromatic), 656 (ωCF_2).

^{1}H-NMR ($CDCl_3$, δ in ppm from TMS): 1.1–2.6 (6.09H, CH_2CH and CH_2CF_2), 3.2–3.9 (15.99H, OCH_3, OCH_2CH_2, $BzOC\underline{H}_2$), 4.2–4.6 (2.59H, $ArC\underline{H}_2O$), 6.2–7.2 (7.97H, aromatic). ^{19}F-NMR ($\underline{C}DCl_3$, δ in

ppm from CF_3CO_2H): −6 (3 F, CF_3), −38 (2 F, CH_2CF_2), −46 to −49 (10 F, CF_2), −51 (2 F, $CF_3C\underline{F}_2$).

Characterization

NMR (^1H, ^{19}F) spectra were recorded with a Varian Gemini VXR 300 spectrometer (operating at 299.9 and 282.2 MHz, respectively).

Size exclusion chromatography (SEC) was carried out with a Jasco PU-1580 liquid chromatograph equipped with two PLgel 5 μm Mixed-D or Mixed-C columns, a Jasco 830-RI refractive index detector and a Perkin Elmer LC75 UV detector. Polystyrene standards ($2 \cdot 10^3$–$1 \cdot 10^6$ Da) were used for calibration.

Differential scanning calorimetry (DSC) measurements were performed with a Mettler DSC-30 instrument (10°C/min). The phase transition temperatures were taken at the maximum temperature in the DSC enthalpic peaks of the second heating cycles. The glass transition temperature was set at the half-devitrification temperature.

Polymer films were prepared by spin-coating 3–5 wt.% polymer solutions in $CHCl_3$ on glass slides followed by annealing for 7 h in a vacuum oven at 120°C.

Static contact angles θ were measured using a Camtel FTA200 contact angle goniometer at room temperature. Water and linear alkanes (Sigma-Aldrich) of the highest purity available were used as standard wetting liquids to evaluate solid surface tension.

XPS spectra were recorded by using a Perkin-Elmer PHI 5600 ci spectrometer with a monochromatic Al-Kα source working at 350 W. The working pressure was less than $1 \cdot 10^{-8}$ Pa. The spectrometer was calibrated by assuming the binding energy (BE) of the Au $4f_{7/2}$ line to be 84.0 eV with respect to the Fermi level. Extended spectra (survey) were collected in the range 0–1350 eV (187.85 eV pass energy, 0.4 eV step, 0.05 s/step). Detailed spectra were recorded for the following regions: C(1s) O(1s) and F(1s) (11.75 eV pass energy, 0.1 eV step, 0.1 s/step).The standard deviation in the BE values of the XPS line was 0.10 eV. The atomic percentage, after a Shirley type background subtraction [8], was evaluated using the PHI sensitivity factors [9]. To take into account charging problems, the C(1s) peak was considered at 285.0 eV and the peak BE differences were evaluated.

RESULTS AND DISCUSSION

Synthesis

The block copolymers were prepared by sequential TEMPO-mediated, controlled radical polymerizations of different styrenic monomers. By

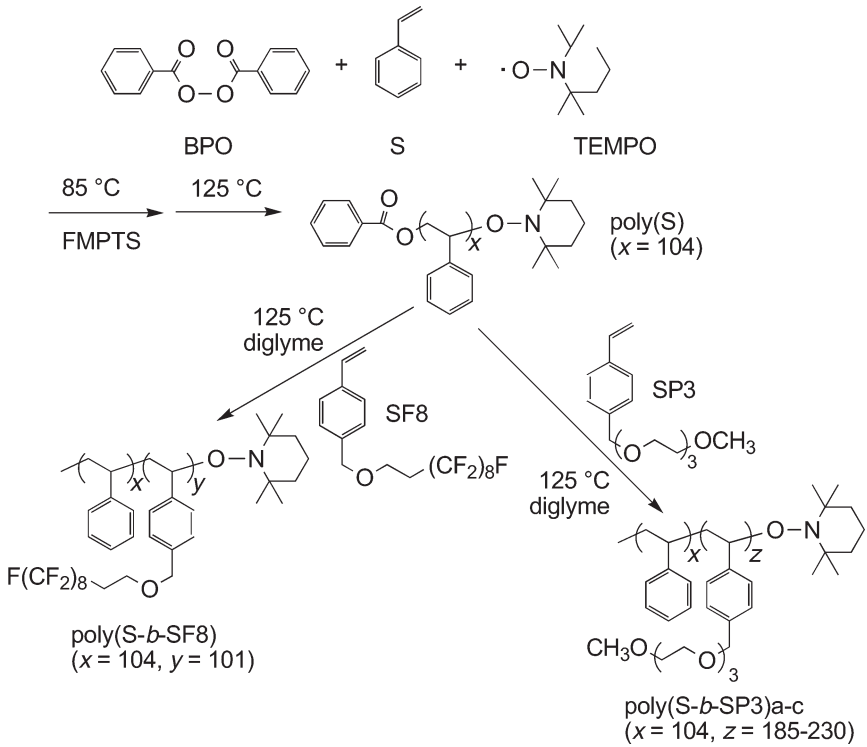

FIGURE 1 Reaction scheme for the TEMPO-mediated preparation of diblock copolymers.

changing the sequence of the monomer addition during the polymerization, triblock copolymers of either the A–B–C or the A–C–B types were obtained. In any case a TEMPO-terminated polystyrene poly(S) was formed as the first block constituent ($x = 104$) with BPO initiation in the presence of FMPTS at 125°C in bulk (Fig. 1). It was then used to polymerize either the semifluorinated styrene SF8 or the PEG-modified styrene SP3 monomers in diglyme solution at 125°C to yield the corresponding diblock copolymers poly(S-*b*-SF8) ($y = 101$) or poly(S-*b*-SP3)a–c ($z = 185$–230).

The TEMPO-terminated diblock copolymers were eventually used to prepare the respective triblock copolymers poly(S-*b*-SF8-*b*-SP3)a–c ($z = 19$–66) and poly(S-*b*-SP3-*b*-SF8)a–c ($y = 49$–146) in diglyme solution at 125°C (Fig. 2).

The formation of block copolymer structures was confirmed by ^{19}F-NMR spectroscopy investigation which clearly proved the insertion of the semifluorinated component in the respective diblock

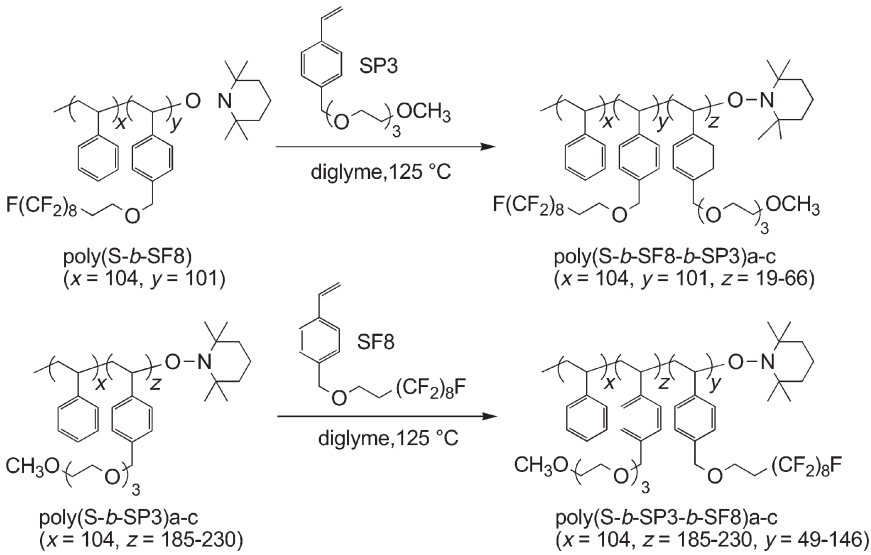

FIGURE 2 Reaction scheme for the TEMPO-mediated preparation of triblock copolymers.

and triblock copolymers (see Experimental Part). While it was easy to incorporate the second block, whether SF8 or SP3, in a predetermined way into diblock copolymers, it was more difficult to grow the third block onto them in a controlled way. This was probably due to the presence of minor amounts of residual dead polymer in the living diblock copolymers used. In consequence, the molar mass distribution of the diblock and the triblock copolymers was relatively broad ($M_w/M_n = 1.2$–1.4).

Thanks to its living character [10], the polymerization procedure adopted led to block copolymers with different macromolecular architectures in which the number-average degrees of polymerization (x, y, and z) greatly varied in a broad compositional range (Table 1). Accordingly, the copolymers contained blocks that were expected to contribute their specific properties of a moderate hydrophobicity (poly(S)), a moderate hydrophilicity (poly(SP3)), and a strong hydrophobicity/lipophobicity (poly(SF8)).

Mesophase Properties

The triblock copolymers presented a complex phase behavior (Table 1). Each of them gave rise to two smectic mesophases, SmF and SmC, with a transition temperature between them at 74–79°C. In no case

TABLE 1 Structural Data[a] and Thermal Transitions[b] of the Triblock Copolymers

Copolymer	Poly(S) block[c] x	Poly(SF8) block y	Poly(SF8) block T_g (°C)	Poly(SF8) block SmF–SmC (°C)	Poly(SP3) block z	Poly(SP3) block T_g (°C)
poly(S-*b*-SF8-*b*-SP3)a	104	101	~58	77	19	~ –58
poly(S-*b*-SF8-*b*-SP3)b	104	101	~57	77	66	~ –65
poly(S-*b*-SF8-*b*-SP3)c	104	101	~58	79	33	–52
poly(S-*b*-SP3-*b*-SF8)a	104	146	~47	78	185	–66
poly(S-*b*-SP3-*b*-SF8)b	104	117	52	75	230	–48
poly(S-*b*-SP3-*b*-SF8)c	104	49	52	74	192	–48

[a]By ^{1}H-NMR and SEC.
[b]By DSC (second heating, 10°C/min).
[c]T_g not detected by DSC.

was the isotropization temperature detected by DSC or visual observation of the low-birefringence textures, and the smectic–isotropic transition temperature was located in the range 110–130°C by wide-angle X-ray diffraction only. A full account of the mesophase structure and sequence of the block copolymers will be given elsewhere.

The glass transition temperature of the poly(S) block, that was expected at about 100°C in analogy with that of the parent polystyrene ($T_g = 104$°C) was indeed not detected. On the other hand, the glass transition of the other poly(SF8) and poly(SP3) block components was easily detected by DSC, even though it spanned over a broad range of temperatures, around 50°C to 60°C and around –50°C to –65°C, respectively, and in some cases its exact value could not be identified. These values compare very well with those of the corresponding homopolymers that were investigated as model compounds for the blocks ($T_g = 50$°C and $T_g = -60$°C, respectively) [10]. Therefore, the overall phase behavior of the triblock copolymers suggests that they were phase separated in a micromorphology (so far unknown) consisting of different one-component domains. Such a microphase separation occurred irrespective of the block interconnections in the A–B–C or A–C–B architectures.

Many previous examples of diblock copolymers containing a liquid crystalline polymer block [11] have proved that a competition can exist between the structuring effects of the liquid crystal mesophase (molecular level) and the domain morphology (supramolecular level) in special, complex structures over different spatial length scales [1]. The present triblock copolymers can provide one more example of such systems, in which multiple interactions operate at the same time.

Wetting Behavior and Surface Energy

The wetting behavior of the polymers was studied by measurements of the static contact angle θ of thin films (200–300 nm thickness) using water and some standard hydrocarbons as the interrogating liquids. The films were spin-coated onto glass slides and then annealed for 7 h at 120°C to achieve equilibrium morphologies.

The values of θ with water and n-hexadecane are conventionally regarded as estimates of hydrophobicity ($\theta_w > \sim 90^\circ$) and lipophobicity ($\theta_h > \sim 60^\circ$), respectively. The measured contact angles for the block copolymers are collected in Table 2. All the triblock copolymers were found to be both hydrophobic ($\theta_w \geq 114^\circ$) and lipophobic ($\theta_h \geq 73^\circ$), because of the preferential surface segregation of the fluorinated block poly(SF8). In fact, the observed values of contact angles were quite similar to those measured for the poly(S-*b*-SF8) diblock copolymer ($\theta_w = 117 \pm 1.2^\circ$, $\theta_w = 78 \pm 0.6^\circ$). In contrast, the poly(S-*b*-SP3) diblock copolymers resulted to be weakly hydrophilic ($\theta_w = 88 \pm 1.6$) but quite lipophilic being completely wetted by n-hexadecane ($\theta_h \sim 0^\circ$).

One also notes that the wetting behavior was virtually identical for the A–B–C and A–C–B triblock copolymers. The low surface energy poly(SF8) block was segregated at the outer polymer/air interface driven there by its lowest surface tension, quite independent of the length of the different blocks and their location in the copolymers. The phenomenon of surface segregation is known for a variety of fluorinated polymers [6,12] and polymer blends [13] and is being pursued as a tool to construct low surface energy, low adhesion polymer coatings.

Measurements of liquid-solid contact angles are commonly used to evaluate solid surface tensions. However, the correlation between θ

TABLE 2 Static Contact Angles with Water and Hexadecane of the Block Copolymers

Polymer	θ_w (°)	θ_h (°)
poly(S)	90 ± 2.0	~ 0
poly(S-*b*-SF8)	117 ± 1.2	78 ± 0.6
poly(S-*b*-SP3)c	88 ± 1.6	~ 0
poly(S-*b*-SF8-*b*-SP3)a	114 ± 0.1	73 ± 0.8
poly(S-*b*-SF8-*b*-SP3)b	117 ± 0.9	76 ± 1.1
poly(S-*b*-SF8-*b*-SP3)c	117 ± 1.4	75 ± 0.9
poly(S-*b*-SP3-*b*-SF8)a	115 ± 1.2	76 ± 1.6
poly(S-*b*-SP3-*b*-SF8)b	114 ± 0.8	78 ± 0.8
poly(S-*b*-SP3-*b*-SF8)c	114 ± 0.3	78 ± 2.1

and γ is still a controversial question and none of the different methods proposed are generally accepted [14,15]. Thus, we followed two alternative approaches to extract the solid surface tension from experimental θ values, namely i) the surface tension component approach, and ii) the equation of state approach. The former was the so-called Owens-Wendt-Kaelble (OWK) approach [16]:

$$\gamma_{LV}(1+\cos\theta) = 2(\gamma_s^d\,\gamma_L^d)^{1/2} + 2(\gamma_s^h\,\gamma_L^h)^{1/2} \quad (1)$$

that regards the surface tension as being composed of two additive components, the dispersive (γ^{d}) and the hydrogen bonding and dipole–dipole (γ^{h}) components, $\gamma = \gamma^{\mathrm{d}} + \gamma^{\mathrm{h}}$. Since there are two unknowns ($\gamma_{\mathrm{S}}^{\mathrm{d}}$ and $\gamma_{\mathrm{S}}^{\mathrm{h}}$) of the solid, it is suggested to use contact angle measurements of at least two different liquids with known $\gamma_{\mathrm{L}}^{\mathrm{d}}$ and $\gamma_{\mathrm{L}}^{\mathrm{h}}$ on one and the same surface by solving two simultaneous equations.

The latter involved the so-called Kwok-Neumann (KN) equation of state [15,17]:

$$\cos\theta = -1 + 2(\gamma_{SV}/\gamma_{LV})^{1/2}\exp[-\beta(\gamma_{LV}-\gamma_{SV})^2] \quad (2)$$

by which, for a given set of liquid surface tension γ_{LV} and θ measured on one and the same solid surface, the constant β and solid surface tension γ_{SV} values can be determined by a least-square analysis technique.

To determine the surface energy of the polymer films by Eq. (1) we investigated their wetting behavior with water ($\gamma_{\mathrm{L}}^{\mathrm{d}} = 21.8\,\mathrm{mJ/m^2}$, $\gamma_{\mathrm{L}}^{\mathrm{h}} = 51.0\,\mathrm{mJ/m^2}$ and several hydrocarbon homologues ($\gamma_{\mathrm{L}}^{\mathrm{h}} = 0$, $\gamma_{LV} = \gamma_{\mathrm{L}}^{\mathrm{d}}$) of varying γ_{LV} such as: n-heptane ($\gamma_{LV} = 20.0\,\mathrm{mJ/m^2}$), n-octane ($\gamma_{LV} = 21.4\,\mathrm{mJ/m^2}$), n-decane ($\gamma_{LV} = 23.9\,\mathrm{mJ/m^2}$), n-dodecane ($\gamma_{LV} = 25.1\,\mathrm{mJ/m^2}$), and n-hexadecane ($\gamma_{LV} = 27.6\,\mathrm{mJ/m^2}$). In our calculations the average $\gamma_{\mathrm{L}}^{\mathrm{d}}$ value of those found for the different hydrocarbons was used.

For the fitting with Eq. (2), we used the same liquids and the literature β value of $1.234 \cdot 10^{-4}\ (\mathrm{m^2/mJ})^2$ as weighted for a variety of solid surfaces [15].

The values of the solid surface energy obtained by the two substantially different methods (Table 3) agreed very well with each other and were consistent with a low surface energy of the polymer films, being comprised in the range of 10–13 $\mathrm{mJ/m^2}$. As expected of non-polar, non-hydrogen bonding surfaces such as fluorinated surfaces, the dispersive contribution $\gamma_{\mathrm{S}}^{\mathrm{d}}$ to γ_{S} was largely dominant, with γ_{S}^{h} being minimal ($\leq 1.3\,\mathrm{mJ/m^2}$). Such a non-zero contribution could be due to the $-CH_2OCH_2-$ moiety of the fluorinated side groups permitting polar interactions with the test liquids [2a].

TABLE 3 Solid Surface Tensions and their Components for the Triblock Copolymers

Copolymer	$\gamma_s^{d\,a}$ (mJ/m^2)	$\gamma_s^{h\,a}$ (mJ/m^2)	$\gamma_s^{OWK\,a}$ (mJ/m^2)	$\gamma_{SV}^{KN\,b}$ (mJ/m^2)
poly(S-*b*-SF8)	10.2	0.7	10.9	10.7
poly(S-*b*-SF8-*b*-SP3)a	11.2	0.9	12.1	11.6
poly(S-*b*-SF8-*b*-SP3)b	10.6	0.6	11.2	11.0
poly(S-*b*-SF8-*b*-SP3)c	10.5	0.5	11.0	11.0
poly(S-*b*-SP3-*b*-SF8)a	11.0	0.7	11.7	11.5
poly(S-*b*-SP3-*b*-SF8)b	10.5	1.1	11.6	11.0
poly(S-*b*-SP3-*b*-SF8)c	10.2	1.3	11.5	10.6

[a]Dispersive and hydrogen bonding and dipole–dipole interaction contributions to the solid surface tension after the Owens-Wendt-Kaelble approach.

[b]Solid surface tension after the Kwok-Neumann equation of state approach ($\beta = 1.234 \cdot 10^{-4}$ (m^2/mJ)^2).

There was basically no influence detectable of the polymer structure on the surface energy in either series of triblock copolymers for any combination of x, y, and z investigated. This finding lends further support to the occurrence of a strong microphase separation of the incompatible blocks, with the fluorinated styrene block being segregated and exposed at the outer interface. The poly(SF8) block was sufficiently long to impose the low surface energy of the films as a result of its distinct hydrophobic and lipophobic character.

The values of the solid surface tensions observed in the present polymers were greater than those previously found ($\gamma_S \sim 6$–8 mJ/m^2) for polyacrylates and polymethacrylates carrying similar semifluorinated chains $-CH_2CH_2(CF_2)_nF$ ($n = 3-10$) [18], by applying a different surface tension component approach, the so-called Lifshitz-van der Waals-van Oss approach [19]. Other than the alternative approach adopted, the differences in surface energetics could be attributed to a perceived greater chain flexibility of the acrylic polymer backbone with respect to the styrenic polymer backbone, which would promote lower surface energy in the former system. However, the two classes of materials could display different molecular organizations at the polymer/air interface.

Surface Analysis

To substantiate better the surface segregation of the fluorinated block we started an analysis of the chemical composition of the film surface by X-ray photoelectron spectroscopy (XPS) measurements. Spectra were recorded at different take-off angles $\alpha = 20^\circ$, 40°, and 70°, that

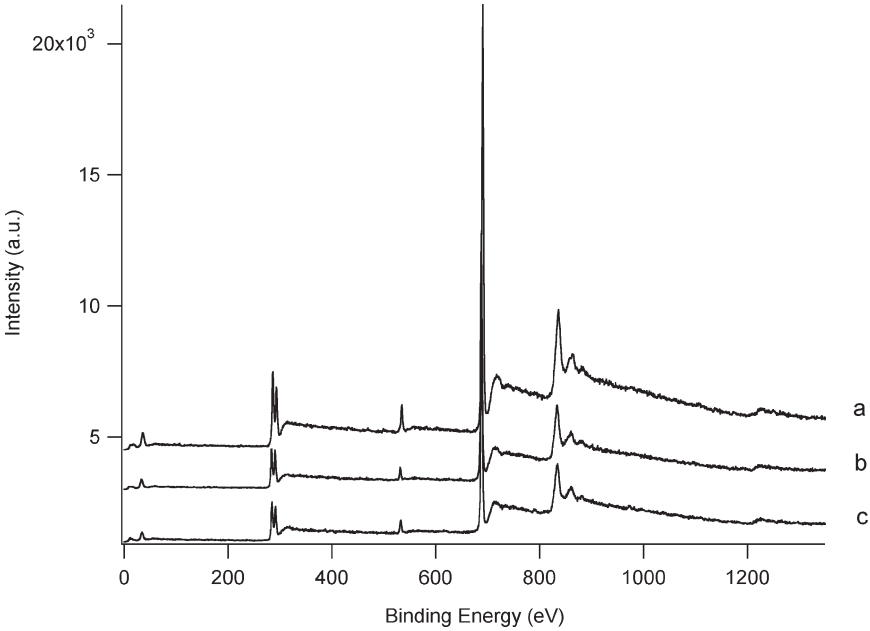

FIGURE 3 XPS survey spectra for diblock copolymer poly(S-b-SF8) (a) and triblock copolymers poly(S-*b*-SF8-*b*-SP3)a (b) and poly(S-*b*-SP3-*b*-SF8)c (c).

corresponded to sampling depths of approximately 30–40 Å, 60–80 Å, and 90–110 Å, respectively.

We focus our attention on the films of poly(S-*b*-SF8-*b*-SP3)a and poly(S-*b*-SP3-*b*-SF8)c that were composed of blocks of very different lengths ($y = 49$ and 101, $z = 192$ and 19, respectively). We also consider diblock copolymer poly(S-*b*-SF8) for comparison. The survey spectra of the three polymers did not show the presence of other elements than C, O and F (Fig. 3).

The C(1s) peak (Fig. 4) revealed a complex shape, and the fitting procedure indicated the presence of several contributions: 284.8 eV (CH), 286.5 eV ($\underline{CH_2}CF_2$ or CH_2O), 289.0 eV (COO), 291.4 eV (CF_2) and 293.7 eV (CF_3). The O(1s) and F(1s) peak positions (533.0 and 689.0 eV, respectively) agreed with what is expected for etheral oxygen and carbon-bound fluorine [20]. Therefore, the chemical analysis of the film surface was qualitatively in agreement with the anticipated structure.

Quantitatively, the elemental analysis data for the different take-off angles α are summarized in Table 4 and compared with the corresponding values calculated from the known stoichiometric ratios of the block components.

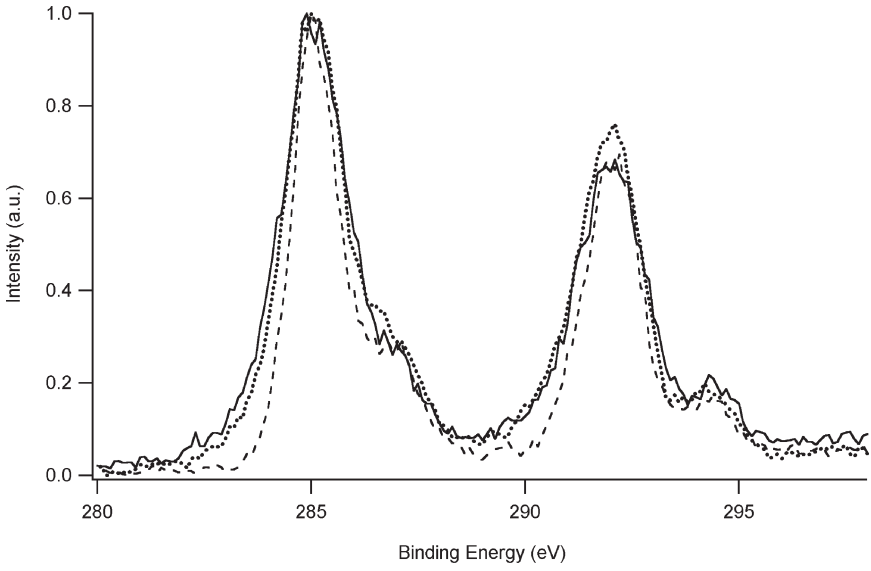

(a)

FIGURE 4 C(1s) XPS spectra obtained at (—) 20°, (·····) 40° and (- - -) 70° for poly(S-*b*-SF8) (a), poly(S-*b*-SF8-*b*-SP3)a (b) and poly(S-*b*-SP3-*b*-SF8)c (c). The spectra were normalized with respect to their value at 285.0 eV.

The atomic percentages changed with angle α, which shows that there was a composition gradient normal to the film surface into the bulk. Specifically, the F atomic percentage decreased with increasing α, that is with the increment of the sampling depth, whereas the C atomic percentage followed the opposite trend. Such variations of composition were more pronounced for the triblock copolymers. For instance, the C composition increased from 45.8% to 51.9% and the F composition decreased from 51.6% to 43.7% in passing from $\alpha = 20^\circ$ to $\alpha = 70^\circ$ for poly(S-*b*-SP3-*b*-SF8)c. Moreover, the experimental F/C ratio was systematically greater than the calculated one for the triblock copolymers at any angle α. Thus, the outermost surface of the polymers films was in all evidence selectively enriched by the low energy fluorinated block.

One can also note that the XPS compositional data of the diblock copolymer poly(S-*b*-SF8) virtually coincided with those calculated by assuming the outer layers to consist exclusively of the fluorinated block poly(SF8), that is C = 51.4%, F = 45.9%, O = 2.7%, with no significant dependence on α. To the same values of composition tended

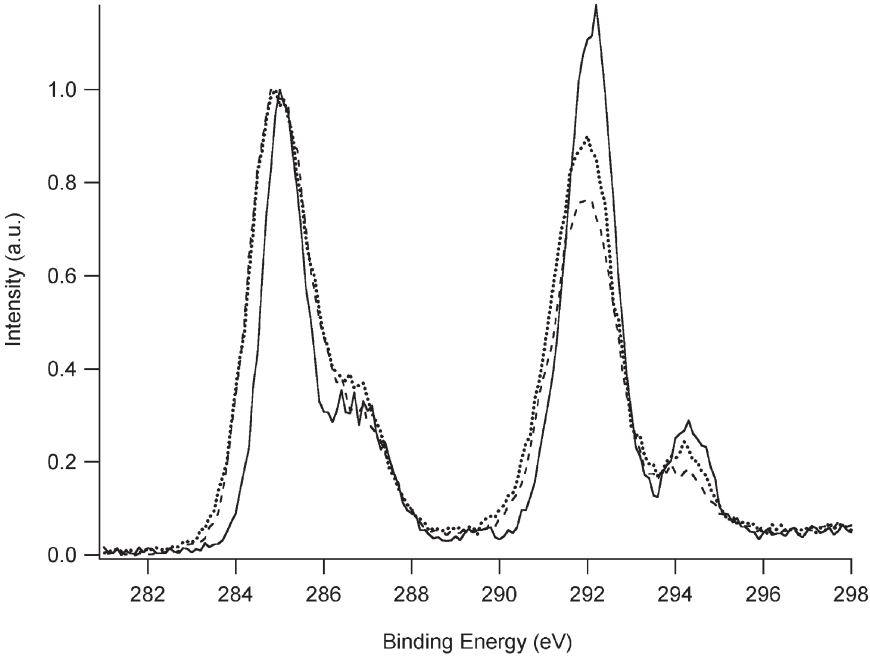

(b)

FIGURE 4 Continued.

the atomic compositions of the triblock copolymers with increasing α, but with opposite trends for C (increasing) and F (decreasing).

The findings on the atomic composition as a function of take-off angle were confirmed by inspection of the C(1s) peak shape. As a matter of fact, the contributions at higher binding energies, due to the C−F bonds, were much more evident at low take-off angles in the triblock copolymers (Fig. 4b and 4c), whereas the peak shape did not change significantly for poly(S-*b*-SF8) (Fig. 4a).

We suggest that the triblock copolymers were more strongly phase separated than the diblock copolymers because of the enhanced mutual incompatibility of the blocks. Moreover, the side groups of poly(SF8) appeared to be ordered and stretched at the polymer/air interface. The length L of the semifluorinated segments in their most extended conformation was calculated to be *ca*. 17 Å. The stretching of the fluorinated segments exposed them at the outer surface [1] and resulted in a low surface energy. In fact, a uniform closed packing of the $-CF_3$ terminals is thought to produce the lowest solid surface tensions [3].

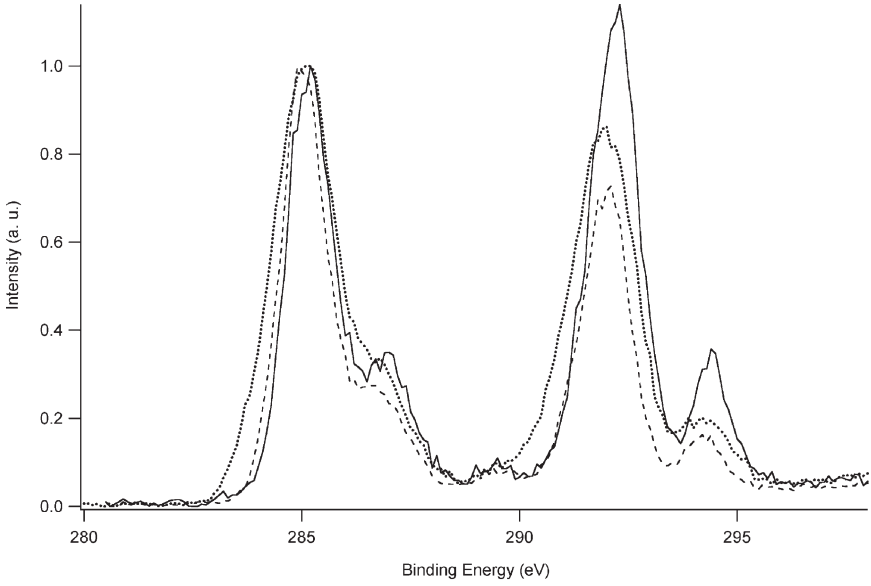

(c)

FIGURE 4 Continued.

The O atomic percentage was very low (2–4%) and its detected variations as a function of take-off angle were not considered suitable for quantitative interpretations. Nonetheless, its gradual rise with α in

TABLE 4 XPS Atomic Composition for the Block Copolymers at Various Take-Off Angles α

Copolymer	α (°)		C (%)	F (%)	O (%)	F/C
poly(S-*b*-SF8)		Calc.[a]	60	38	2	0.63
	20	Exp.	49.9	46.8	3.3	0.94
	40		51.5	44.8	3.7	0.87
	70		51.3	44.9	3.8	0.88
poly(S-*b*-SP3-*b*-SF8)c		Calc.[a]	74	13	13	0.18
	20	Exp.	45.8	51.6	2.6	1.13
	40		49.8	47.4	2.8	0.95
	70		51.9	43.7	4.4	0.84
poly(S-*b*-SF8-*b*-SP3)a		Calc.[a]	62	35	3	0.56
	20	Exp.	44.8	52.7	2.5	1.18
	40		49.0	48.1	2.9	0.98
	70		50.8	45.9	3.3	0.90

[a]Calculated on the basis of the known degrees of polymerization x, y, and z.

the triblock copolymers may indicate the growing contribution from the poly(SP3) block next to the surface and underlying the poly(SF8) block.

CONCLUSION

The investigated block copolymers formed the mesophases typical for the semifluorinated polymer block, thanks to the microphase separation of the incompatible block components. Moreover, the low energy fluorinated block was preferentially surface segregated regardless of the type of block sequencing. These phenomena were enhanced with respect to the parent diblock copolymers because of the further increased incompatibility of the different blocks. Thus, the design of macromolecular architectures can make different structuring effects cooperate in one material to provide special bulk and surface properties, including low surface energy behavior.

REFERENCES

[1] Li, X., Andruzzi, L., Chiellini, E., Galli, G., Ober, C. K., Hexemer, A., Kramer, E. J., & Fischer, D. A. (2002). *Macromolecules*, *35*, 8078.
[2] For very recent and diverse examples, see
(a) Bertolucci, M., Galli, G., Chiellini, E., & Wynne, K. J. (2004). *Macromolecules*, *37*, 3666.
(b) Granville, A. M. & Brittain, W. J. (2004). *Macromol. Rapid Commun.*, *25*, 1298.
(c) Bongiovanni, R., Malucelli, G., Sangermano, M., & Priola, A. (2004). *J. Fluorine Chem.*, *125*, 345.
[3] Wang, J., Mao, G., Ober, C. K., & Kramer, E. J. (1997). *Macromolecules*, *30*, 1906, and references therein.
[4] (a) Ragnoli, M., Pucci, E., Bertolucci, M., Gallot, B., & Galli, G. (2004). *J. Fluorine Chem.*, *125*, 283.
(b) Galli, G., Ragnoli, M., Bertolucci, M., Ober, C. K., Kramer, E. J., & Chiellini, E. (2004). *Macromol. Symp.*, *218*, 303.
[5] Galli, G., Andruzzi, L., Chiellini, E., Li, X., Ober, C. K., Hexemer, A., & Kramer, E. J. (2004). *Surf. Coat. Internat., Part B, Coat. Trans.*, *87*, 77.
[6] Höpken, J. & Möller, M. (1992). *Macromolecules*, *25*, 1461.
[7] Andruzzi, L., Senaratne, W., Hexemer, A., Ober, C. K., & Kramer, E. J. (2003). *Amer. Chem. Soc., Polym. Mater. Sci. Eng. Div.*, *88*, 604.
[8] Shirley, D. A. (1972). *Phys. Rev.*, *55*, 4709.
[9] Moulder, J. F., Stickle, W. F., Sobol, P. E., & Bomben, K. D. (1992). In: *Handbook of X-ray Photoelectron Spectroscopy*, J. Chastain, (Ed.), Physical Electronics: Eden Prairie, MN.
[10] Andruzzi, L., Chiellini, E., Galli, G., Li, X., Kang, S. H., & Ober, C. K. (2002). *J. Mater. Chem.*, *12*, 1684, and references therein.
[11] (a) Klok, H.-A. & Lecommandoux, S. (2001). *Adv. Mater.*, *13*, 1217.
(b) Galli, G. (1997). *Macromol. Symp.*, *117*, 109.
[12] (a) Pospiech, D., Jehnichen, D., Gottwald, A., Häussler, L., Kollig, W., Grundke, K., Janke, A., Schmidt, S., & Werner, C. (2003). *Surf. Coat. Internat., Part B: Coat. Trans.*, *86*, 43.

(b) Perutz, S., Dai, C.-A., Ober, C. K., & Kramer, E. J. (1996). *Macromolecules*, *29*, 1229.
[13] (a) Casazza, E., Mariani, A., Ricco, L., & Russo, S. (2002). *Polymer*, *43*, 1207.
(b) Iyengar, D. R., Perutz, S. M., Wang, J., Kramer, E. J., Ober, C. K., & Ellis, K. (1998). *Macromolecules*, *31*, 4272.
[14] (a) Della Volpe, C., Maniglio, D., Brugnara, M., Siboni, S., & Morra, M. (2004). *J. Colloid Interface Sci*., *271*, 434.
(b) Siboni, S., Della Volpe, C., Maniglio, D., & Brugnara, M. (2004). *J. Colloid Interface Sci*., *271*, 454.
[15] Kwok, D. Y. & Neumann, A. W. (1999). *Adv. Colloid Interface Sci*., *81*, 167.
[16] (a) Owens, D. K. & Wendt, R. C. (1969). *J. Appl. Polym. Sci*., *13*, 1741.
(b) Kaelble, D. H. (1970). *J. Adhesion*, *2*, 66.
[17] Li, D. & Neumann, A. W. (1990). *J. Colloid Interface Sci*., *137*, 304.
[18] Tsibouklis, J. & Nevell, T. G. (2003). *Adv. Mater*., *15*, 647.
[19] van Oss, C. J., Chaudury, M. K., & Good, R. J. (1988). *Chem. Rev*., *88*, 927.
[20] (a) Fadley, C. S., Bergström, S. Å. L. Shirley, D. A. (Ed.), (1972). In: *Electron Spectroscopy*, North-Holland: Amsterdam.
(b) *X-ray Photoelectron Spectroscopy Database* 20, Version 3.0, National Institute of Standards and Technology, Gaithersburg, MD.